

Highly Luminescent, Visible-Emitting Lanthanide Macrocyclic Chelates Stable in Water and Derived from the Cyclen Framework

Gaël Zucchi, Anne-Claire Ferrand, Rosario Scopelliti, and Jean-Claude G. Bünzli*

Swiss Federal Institute of Technology Lausanne, Institute of Molecular and Biological Chemistry, BCH 1402, CH-1015-Lausanne, Switzerland

Received October 31, 2001

Two new tetraazamacrocyclic ligands are designed with the aim of sensitizing the luminescence of Tb(III) and Eu(III) ions in water: **L5** {1,4,7,10-tetrakis[*N*-(phenacyl)carbamoylmethyl]-1,4,7,10-tetraazacyclododecane} and **L6** {1,4,7,10-tetrakis[*N*-(4-phenylphenacyl)carbamoylmethyl]-1,4,7,10-tetraazacyclododecane}. These ligands react with lanthanide trifluoromethanesulfonates to yield stable 1:1 complexes in water ($\log K = 12.89 \pm 0.15$ for **EuL5**). X-ray diffraction on [Tb(**L5**)(H₂O)](CF₃SO₃)₃ ($P\bar{1}$, $a = 13.308(3)$ Å, $b = 14.338(3)$ Å, $c = 16.130(3)$ Å, $\alpha = 101.37(3)^\circ$, $\beta = 96.16(3)^\circ$, $\gamma = 98.60(3)^\circ$) shows the Tb(III) ion lying on a C_4 axis and being 9-coordinate, with one water molecule bound in its inner coordination sphere. The absolute quantum yields are determined in aerated water for the complexes formed with ions used in fluoroimmunoassays (Ln = Sm, Eu, Tb, and Dy). Large values are found for [Tb(H₂O)(**L5**)]³⁺ and [Eu(H₂O)(**L6**)]³⁺, in line with the molecular design of the receptors: 23.1% and 24.7%, respectively. The intense luminescence of these ions results from efficient intersystem crossing and L → Ln energy transfer processes, as well as from a suitable shielding of the emitting ions from radiationless deactivation.

Introduction

Luminescent lanthanide complexes are increasingly used as diagnostic tools in biomedical analysis, as responsive analytical systems,¹ as luminescent labels for enhanced imaging of cancer² or for fluoroimmunoassays,³ and in color-tailored fluorophores for simultaneous detection of multiple targets on DNA strands.^{4,5} Encapsulating the lanthanide ions into suitable receptors able to sensitize their luminescence and to provide thermodynamically stable and kinetically inert edifices under physiological conditions is a challenge that chemists have addressed in several ways.^{6,7} Among them, the use of a cyclen framework (cyclen is 1,4,7,10-tetraazacyclododecane) fitted with functionalized dangling arms has proved to be quite successful for the design of Gd-containing contrast agents for magnetic resonance imaging⁸ and su-

pramolecular assemblies with enhanced physicochemical properties,⁹ as well as for selective luminescent signaling of various analytes including pH.^{1,10}

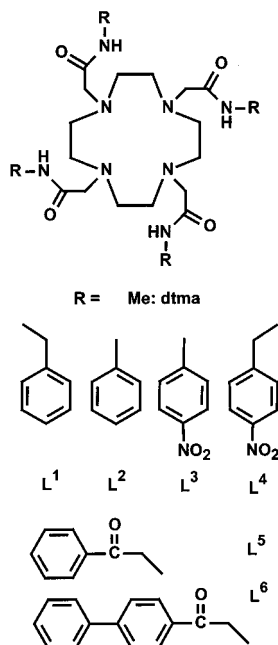
We have shown that a cyclen-based ligand fitted with carbamoyl pendant arms (**L1**, see Chart 1) leads to stable lanthanide chelates with pseudo C_4 symmetry and that the luminescence of Tb(III) is fairly well sensitized.¹¹ More recently, a detailed photophysical study of the complexes with **L1–L4** associated with structural investigations demonstrated the importance of the various parameters intervening in sensitizing the luminescence of Ln(III) ions.¹² In particular, **L1** and **L4**, which feature a methylene spacer between the aromatic chromophoric unit and the amide binding moiety, are much better sensitizers of the Tb(III) luminescence than, respectively, **L2** and **L3**, which are devoid of this characteristic, because the chromophoric unit

* To whom correspondence should be addressed. E-mail: jean-claude.bunzli@epfl.ch.

- (1) Parker, D. *Coord. Chem. Rev.* **2000**, *205*, 109.
- (2) Bornhop, D. J.; Hubbard, D. S.; Houlne, M. P.; Adair, C.; Kiefer, G. E.; Pence, B. C.; Morgan, D. L. *Anal. Chem.* **1999**, *71*, 2607.
- (3) Yam, V. W. W.; Lo, K. K. W. *Coord. Chem. Rev.* **1999**, *184*, 157.
- (4) Chen, J. Y.; Selvin, P. R. *J. Am. Chem. Soc.* **2000**, *122*, 657.
- (5) Xiao M.; Selvin, P. R. *J. Am. Chem. Soc.* **2001**, *123*, 7067.
- (6) Bünzli, J.-C. G.; André, N.; Elhabiri, M.; Muller, G.; Piguet, C. J. *Alloys Compd.* **2000**, *303/304*, 66.
- (7) Piguet, C.; Bünzli, J.-C. G. *Chem. Soc. Rev.* **1999**, *28*, 347.

- (8) Caravan, P.; Ellison, J. J.; McMurry, T. J.; Lauffer, R. B. *Chem. Rev.* **1999**, *99*, 2293.
- (9) Skinner, P. J.; Beeby, A.; Dickins, R. S.; Parker, D.; Aime, S.; Botta, M. *J. Chem. Soc., Perkin Trans. 2* **2000**, 1329.
- (10) Lowe, M. P.; Parker, D.; Reany, O.; Aime, S.; Botta, M.; Castellano, G.; Gianolio, E.; Pagliarin, R. *J. Am. Chem. Soc.* **2001**, *123*, 7601.
- (11) Zucchi, G.; Scopelliti, R.; Pittet, P. A.; Bünzli, J.-C. G.; Rogers, R. D. *J. Chem. Soc., Dalton Trans.* **1999**, 931.
- (12) Zucchi, G.; Scopelliti, R.; Bünzli, J.-C. G. *J. Chem. Soc., Dalton Trans.* **2001**, 1975.

Chart 1



can less favorably position itself above the metal ion. However, mainly because of unfavorable energy factors for Tb(III) and photoelectron-transfer processes for Eu(III), the quantum yield of the $[\text{LnL}]^{3+}$ ($i = 1-4$) complexes is too low for utilizing them as efficient luminescent stains. Because phenacyl and 4-phenylphenacyl chromophores are known to induce efficient energy transfers onto Tb(III) and Eu(III) ions,¹³ we have now designed ligands **L5** and **L6** incorporating these moieties. In this paper, we describe the synthesis of these receptors and of the resulting complexes; we show that not only Eu(III) and Tb(III) give rise to highly luminescent compounds but that the luminescence of Sm(III) and Dy(III) can also be sensitized. In addition, we report the first X-ray structure of a Tb(III) complex derived from cyclen as well as the stability constant of the Eu(III) complex with **L5** in aqueous solution.

Experimental Section

General. Solvents and chemicals were purchased from Fluka AG (Buchs, Switzerland). Acetonitrile was dried over CaH_2 and P_2O_5 .¹⁴ Dichloromethane and tetrahydrofuran were distilled from CaH_2 . Lanthanide trifluoromethanesulfonates (triflates, trif) were prepared from the oxides (Rhône-Poulenc, 99.99%) and triflic acid,¹⁵ while dtma¹⁶ and cyclen¹⁷ have been synthesized according to literature procedures. Elemental analyses were carried out by Dr. H. Eder from the Microchemical Laboratory of the University of Geneva.

Spectroscopic Measurements. Electrospray mass spectra (ES-MS) were measured on a Finnigan SSQ-710C spectrometer driven

by a Digital Personal DEC station 5000/25. NMR spectra were recorded on Bruker AM-360 (360.16 MHz) or Avance DRX-400 (400.03 MHz) spectrometers. Proton chemical shifts are reported in parts per million (ppm) with respect to TMS. Electronic spectra in the UV-vis range were recorded at 293 K using a Perkin-Elmer Lambda 900 spectrometer connected to an external computer and using quartz cells of 1.000 cm path length (Hellma). The concentration of the solutions ranged from 1×10^{-4} to 1×10^{-7} M. IR spectra were collected on an FT-IR Mattson Alpha Centauri spectrometer (KBr pellets). Low-resolution luminescence measurements were made on a Perkin-Elmer LS-50B spectrofluorimeter. High-resolution spectra and lifetimes (averages of at least four determinations) of the Eu(III) complexes in the solid state were measured on a previously described instrumental setup.¹⁸

Syntheses. **N-(Phenacyl)bromoacetamide (1).** Phenacylamine hydrochloride (1.000 g, 5.8 mmol) in CH_2Cl_2 was added to an aqueous solution of NaOH (0.466 g, 11.7 mmol). The mixture was cooled to 273 K, and bromoacetyl bromide (0.569 mL, 5.8 mmol) was added dropwise. The resulting solution was stirred for 30 min at 273 K and for 1½ h at room temperature. The aqueous phase was extracted with 4×10 mL of CH_2Cl_2 , and the organic phase was washed with 3×50 mL of H_2O , dried on Na_2SO_4 , and evaporated under vacuum. The residue was recrystallized in a 1/1 hexane/ethyl acetate mixture (0.740 g, 2.9 mmol, 50%). Calcd for $\text{C}_{10}\text{H}_{10}\text{O}_2\text{NBr}$: C, 46.90; H, 3.94; N, 5.47. Found: C, 46.77; H, 3.99; N, 5.48. δ_{H} (CDCl_3 , 293 K): 3.96 (s, 2H, NCH_2CO), 4.78 (d, $^2J = 4.2$ Hz, 2H, NCH_2COPh), 7.52 (t, $^2J = 7.6$ Hz, 2H, Ph), 7.60 (br, 1H, NH), 7.65 (t, $^2J = 7.6$ Hz, 1H, Ph), 7.99 (d, $^2J = 7.6$ Hz, 2H, Ph).

1,4,7,10-Tetrakis[*N*-(phenacyl)carbamoylmethyl]-1,4,7,10-tetraazacyclododecane (L5). A mixture of cyclen (0.050 g, 0.3 mmol) and **1** (0.334 g, 1.3 mmol) was refluxed for 6 h in dry THF containing NEt_3 (0.324 mL, 2.3 mmol). A white precipitate formed which was washed with water and recrystallized in CH_3CN (0.148 g, 0.17 mmol, 57%). Calcd for $\text{C}_{48}\text{H}_{56}\text{O}_8\text{N}_8$: C, 66.04; H, 6.47; N, 12.84. Found: C, 65.82; H, 6.28; N, 12.63. $m/z = 873.8$ ($[\text{HL5}]^+$) and 437.3 ($[\text{H}_2\text{L5}]^{2+}$). δ_{H} (CD_3CN , 293 K): 2.97 (s, 4 H, NCH_2cycle), 3.54 (s, 2 H, NCH_2CO), 4.48 (d, $^2J = 5.3$ Hz, 2H, NCH_2COPh), 7.44 (t, $^2J = 7.6$ Hz, 2H, Ph), 7.60 (t, $^2J = 7.6$ Hz, 1H, Ph), 7.64 (t, 1H, NH), 7.80 (dd, $^2J = 7.6$ Hz, $^3J = 1.2$ Hz, 2H, Ph). $\nu_{\text{max}} = 3311$ (N—H), 1700 (C=O_{Ph}), 1663 (C=ONH) cm^{-1} .

4-Phenylphenacylamine (2).¹⁹ Sodium diformylamide (0.415 g, 4.3 mmol) was added to a solution of 4-phenylphenacyl bromide (1 g, 3.6 mmol) in CH_2Cl_2 . The resulting solution was stirred for 2 h at 343 K, filtrated, and washed with 10 mL of hot CH_3CN , and half of the solvent was evaporated; **2** crystallized directly from this solution (0.684 g, 3.2 mmol, 90%). δ_{H} ($\text{DMSO}-d_6$, 293 K): 4.64 (s, 2H, COCH_2), 7.47 (q, 1H, Ar), 7.53 (t, 2H, Ar), 7.78 (d, $^2J = 6.5$ Hz, 2H, Ar), 7.91 (d, $^2J = 8.6$ Hz, 2H, Ar), 8.11 (d, $^2J = 8.6$ Hz, 2H, Ar), 8.38 (br, 2H, NH_2).

4-Phenylphenacylamine Hydrochloride (3). A 10 mL portion of a 5% HCl solution in EtOH was added to **2** (0.610 g, 2.9 mmol). The resulting solution was stirred for 24 h at room temperature and then evaporated. The beige solid was washed with 5 mL of Et_2O and dried (0.720 g, 2.9 mmol, 90%).

***N*-(4-Phenylphenacyl)-bromoacetamide (4).** Compound **3** (0.500 g, 2.0 mmol) was dissolved in 50 mL of CH_2Cl_2 and added to an aqueous solution of NaOH (0.160 g, 4.0 mmol). The solution was cooled to 273 K, and bromoacetyl bromide (0.170 mL, 2.0 mmol) in CH_2Cl_2 was added dropwise under vigorous stirring. The mixture

(13) Sato, N.; Shinkai, S. *J. Chem. Soc., Perkin Trans. 2* **1993**, 621.
 (14) Perrin, D. D.; Armarego, W. L. F. *Purification of Laboratory Chemicals*; Pergamon Press: Oxford, 1988.
 (15) Bünzli, J.-C. G.; Pilloud, F. *Inorg. Chem.* **1989**, *28*, 2638.
 (16) Alderighi, L.; Bianchi, A.; Calabi, L.; Dapporto, P.; Giorgi, C.; Losi, P.; Paleari, L.; Paoli, P.; Rossi, P.; Valtancoli, B.; Virtuani, M. *Eur. J. Inorg. Chem.* **1998**, 1581.
 (17) Pittet, P. A.; Fruh, D.; Tissières, V.; Bünzli, J.-C. G. *J. Chem. Soc., Dalton Trans.* **1997**, 895.

(18) Bünzli, J.-C. G.; Milicic-Tang, A. *Inorg. Chim. Acta* **1996**, *252*, 221.
 (19) Yinglin, H.; Hongwen, H. *Synthesis* **1990**, *7*, 615.

was then stirred for 30 min at 273 K and for 1½ h at room temperature. The aqueous phase was extracted with 4 × 10 mL of CH₂Cl₂, and the organic phase was washed with 50 mL of water, dried on Na₂SO₄, and evaporated under vacuum. The crude product was recrystallized in a 1/1 hexane/ethyl acetate mixture (0.864 g, 2.6 mmol, 90%). Calcd for C₁₆H₁₄N₂O₂Br: C, 57.85; H, 4.25; N, 4.22. Found: C, 58.10; H, 4.29; N, 4.18. δ_{H} (CDCl₃, 293 K): 3.98 (s, 2H, NCH₂), 4.82 (d, $^2J = 3.8$ Hz, 2H, BrCH₂), 7.43 (m, 1H, Ar), 7.49 (t, $^2J = 7.7$ Hz, 2H, Ar), 7.57 (br, 1H, NH), 7.64 (d, $^2J = 7.7$ Hz, 2H, Ar), 8.06 (d, $^2J = 7.7$ Hz, 2H, Ar).

1,4,7,10-Tetrakis[*N*-(4-phenylphenacyl)carbamoylmethyl]-1,4,7,10-tetraazacyclododecane (L6). Compound **4** (0.864 g, 2.6 mmol) was added to a solution of cyclen (0.099 g, 0.58 mmol) in 40 mL of anhydrous THF containing NEt₃ (0.349 mL, 2.6 mmol). The mixture was refluxed for 12 h and filtrated. The beige solid was washed with 50 mL of water, stirred for 2 h in 50 mL of hot CH₃CN, filtrated, and dried (0.588 g, 0.5 mmol, 88%). Calcd for C₇₂H₇₂N₈O₈: C, 73.45; H, 6.16; N, 9.52. Found: C, 73.72; H, 6.32; N, 9.31. $m/z = 1177.8$ ([HL6]⁺) and 589.9 ([H₂L6]²⁺). δ_{H} (DMSO-*d*₆, 293 K): 3.35 (s, 4H, NCH₂), 4.05 (s, 2H, NCH₂CO), 4.74 (d, $^2J = 5.3$ Hz, 2H, NCH₂COAr), 7.43–7.63 (m, 3H, Ar), 7.79 (d, $^2J = 7.8$ Hz, 2H, Ar), 7.88 (d, $^2J = 7.7$ Hz, 2H, Ar), 8.11 (d, $^2J = 7.7$ Hz, 2H, Ar), 8.69 (t, 1H, NH). $\nu_{\text{max}} = 3310$ (N–H), 1697 (C=OPh), 1650 (C=ONH) cm⁻¹.

Preparation of the Complexes. Lanthanide complexes of **L5** and **L6** were isolated with triflates as counterions. They were prepared by heating 1 equiv of the Ln salt and 1 equiv of L at reflux in dry acetonitrile for 24 h. After cooling, the solution was filtered on sintered glass and concentrated; CH₂Cl₂ was added to the solution which was kept overnight at 277 K. The deposited solid was recovered by filtration, washed with CH₂Cl₂, and dried for 2 h at 313 K under vacuum (1 mbar). The complexes with **L5** were recrystallized from water, and those with **L6**, from CH₃CN. Yields ranged between 60% and 70%. **SmL5·2H₂O (5)**. Calcd for SmC₅₁H₆₀O₁₉N₈S₃F₉: C, 40.66; H, 4.01; N, 7.44. Found: C, 40.84; H, 4.14; N, 7.43. **EuL5 (6)**. Calcd for EuC₅₁H₅₆O₁₇N₈S₃F₉: C, 41.61; H, 3.83; N, 7.61. Found: C, 41.99; H, 4.23; N, 7.78. **TbL5·2H₂O (7)**. Calcd for TbC₅₁H₆₀O₁₉N₈S₃F₉: C, 40.43; H, 3.99; N, 7.40. Found: C, 40.65; H, 4.12; N, 7.40. **DyL5·2H₂O (8)**. Calcd for DyC₅₁H₆₀O₁₉N₈S₃F₉: C, 40.33; H, 3.98; N, 7.38. Found: C, 40.29; H, 4.08; N, 7.36. **LuL5·3H₂O (9)**. Calcd for LuC₅₁H₆₂O₂₀N₈S₃F₉: C, 40.31; H, 4.34; N, 7.10. Found: C, 40.25; H, 4.26; N, 7.31. **SmL6 (10)**. Calcd for SmC₇₅H₇₄O₁₈N₈S₃F₉: C, 50.75; H, 4.09; N, 6.31. Found: C, 50.68; H, 4.62; N, 5.66. **EuL6·H₂O (11)**. Calcd for EuC₇₅H₇₆O₁₉N₈S₃F₉: C, 50.20; H, 4.16; N, 6.24. Found: C, 49.93; H, 4.41; N, 5.97. **TbL6 (12)**. Calcd for TbC₇₅H₇₄O₁₈N₈S₃F₉: C, 50.00; H, 4.14; N, 6.22. Found: C, 49.71; H, 4.41; N, 6.06. **LuL6·3H₂O (13)**. Calcd for LuC₇₅H₈₂O₂₂N₈S₃F₉: C, 48.13; H, 4.31; N, 5.99. Found: C, 48.53; H, 4.45; N, 5.92.

Stability Constant Determination. The stability constant of **EuL5** was determined at 298 K by competitive titration with dtma (1,4,7,10-tetrakis(methylcarbamoylmethyl)-1,4,7,10-tetraazacyclododecane); log $K(\text{Eu}) = 13.17 \pm 0.04$ in H₂O containing 0.1 M Me₄NNO₃ at 298.1 K,¹⁶ where K is the constant of the equilibrium [Eu(H₂O)_{*n*}]³⁺ + L ⇌ [Eu(H₂O)(L)]³⁺ + (*n*–1)H₂O. As the complex formation for [EuL]³⁺ (L = dtma, **L5**) is slow, it was necessary to operate in batch mode, and 30 individual solutions were prepared at pH 6.5. Each solution was made up of a mixture of 5 mL of **L5** (6 × 10⁻⁵ M), 5 mL of dtma (6 × 10⁻⁵ M), and various amounts of Eu(trif)₃·5H₂O (1.2 × 10⁻⁴ M). The ratio [Eu]₀/([dtma]₀ + [L]₀) varied between 0 and 1.5, and the ionic strength was adjusted to 0.1 M with Me₄NNO₃. The solutions were equilibrated for 25 days at 298 K in a thermostated bath. The collected data were analyzed

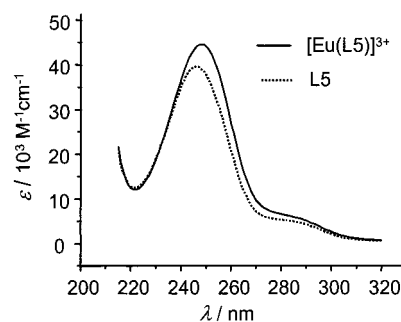


Figure 1. Absorption spectra of **L5** and **EuL5** in water.

Table 1. Absolute Quantum Yields (%) of **EuL5** and **EuL6** Relative to Cresyl Violet (CV), Rhodamine 101 (RH), and **EuL6**, as a Function of the Excitation Energy

$E_{\text{exc}}/$ cm^{-1} :	EuL5			EuL6		
	40 320	37 740	34 720	40 320	37 740	34 720
$Q(\text{CV})$	2.1	2.5	6.4	8.4	16.7	24.5
$Q(\text{RH})$	2.1	2.6	5.2	12.8	18.9	24.9
$Q(\text{EuL6})$	(1.6) ^a	(5.2) ^a	5.0			
Q_{CV}^b	54.6	56.8	43.6	47.0	60.8	48.1

^a Unreliable data due to very low absorption of **L6** at these wavenumbers.

^b Absolute quantum yield of CV relative to RH, recalculated from the data on EuL (literature value: 54%).²¹

with SPECFIT;²⁰ the factor analysis revealed two absorbing species, **L5** and **EuL5**, the spectra of which are very similar, but for a slight increase in molar absorption coefficient for the latter (Figure 1).

Quantum Yields Measurements. All the quantum yields Q have been measured in aerated water and calculated using the equation $Q_x/Q_r = A_r(\tilde{\nu}) \cdot n_x^2 \cdot D_x / A_x(\tilde{\nu}) \cdot n_r^2 \cdot D_r$, where x refers to the sample, and r , to the reference; A is the absorbance, $\tilde{\nu}$, the excitation wavenumber used, n , the refractive index, and D , the integrated emitted intensity. Measurements on the Eu(III) complexes were performed using two organic references emitting in the same region as Eu(III), cresyl violet (CV, $Q_{\text{abs}} = 54\%$ in methanol)²¹ and rhodamine 101 (RH, $Q_{\text{abs}} = 100\%$ in ethanol).²¹ Such an experimental procedure allowed us to calculate the quantum yield of one reference relative to the other in order to check the consistency of the data (Table 1). The values found are close to the literature data, within the experimental error which is estimated to be ±20%. Three different excitation energies have been used: 40 320 cm⁻¹ (maximum of the $\pi \rightarrow \pi^*$ transition of complexed **L5**), 37 740 cm⁻¹ (an energy at which the absorption spectra of the two references present a maximum), and 34 720 cm⁻¹ (maximum of absorption of **EuL6**). For the complexes, all the ⁵D₀ → ⁷F_J transitions were taken into account ($J = 0-6$): transitions to $J = 5$ and 6 account for 9% and 23% of the total emission of **EuL5** and **EuL6**, respectively. In addition, the quantum yield of **EuL5** was measured taking **EuL6** as reference, and the value found was the same as that obtained with the organic references (Table 1). The EuL complexes were taken as references for the determination of $Q(\text{SmL})$, while the quantum yields of **TbL5** and **TbL6** were measured relative to quinine sulfate (QS, $Q_{\text{abs}} = 54.6\%$ in 0.5 M aqueous H₂SO₄) and to 9, 10-diphenylanthracene (DPA, $Q_{\text{abs}} = 90\%$ in cyclohexane) and **TbL5** for **DyL5** (Table 2). The refractive indices were equal to 1.338, 1.425, 1.328, 1.360, and 1.332 for solutions of QS, DPA, CS, RH, and of the LnL complexes, respectively. Samples have

(20) Gampp, H.; Maeder, M.; Meyer, C. J.; Zuberbühler, A. D. *Talanta* **1986**, *33*, 943.

(21) Eaton, D. F. *Pure Appl. Chem.* **1988**, *60*, 1107.

Table 2. Absolute Quantum Yields (%) of LnL5 (Ln = Sm, Tb, Dy) and LnL6 (Ln = Sm, Tb)

cmpd	E_{exc}/cm^{-1}	ref ^a	$Q/\%$	cmpd	E_{exc}/cm^{-1}	ref ^a	$Q/\%$	
SmL5	40 320	EuL1	0.061	SmL6	40 320	EuL5	0.36	
	37 740		0.16		34 720		EuL5	0.50
	34 720		0.40		34 720		EuL6	0.70
TbL5	40 320	QS	23.1	TbL6	34 720	QS	1.0	
DyL5	40 320	QS	0.06					
		DPA	0.05					
		TbL5	0.04					

^a See Experimental Section.

Table 3. Crystal Data and Details for the Structure Determination of **TbL5**

chemical formula	[C ₄₈ H ₅₈ N ₈ O ₉ Tb][(CF ₃ O ₃ S)] ₃ ·2H ₂ O
fw	1533.19
cryst syst	triclinic
space group	<i>P</i> 1
<i>a</i> (Å)	13.308(3)
<i>b</i> (Å)	14.338(3)
<i>c</i> (Å)	16.130(3)
α (deg)	101.37(3)
β (deg)	96.16(3)
γ (deg)	98.60(3)
vol (Å ³)	2953.5(10)
<i>Z</i>	2
D_{calcd} (g cm ⁻³)	1.724
$F(000)$	1556
μ (mm ⁻¹)	1.415
temp (K)	143
wavelength (Å)	0.710 70
measured reflns	15 797
unique reflns	9262
unique reflns [$I > 2\sigma(I)$]	6503
data/params	9262/830
R^a [$I > 2\sigma(I)$]	0.0650
wR2 ^a (all data)	0.1872
GOF	0.984

^a $R = \sum ||F_o| - |F_c|| / \sum |F_o|$; wR2 = $\{\sum [w(F_o^2 - F_c^2)^2] / \sum [w(F_o^2)^2]\}^{1/2}$.

^b GOF = $\{\sum [w(F_o^2 - F_c^2)^2] / (n - p)\}^{1/2}$ where *n* is the number of data and *p* is the number of parameters refined.

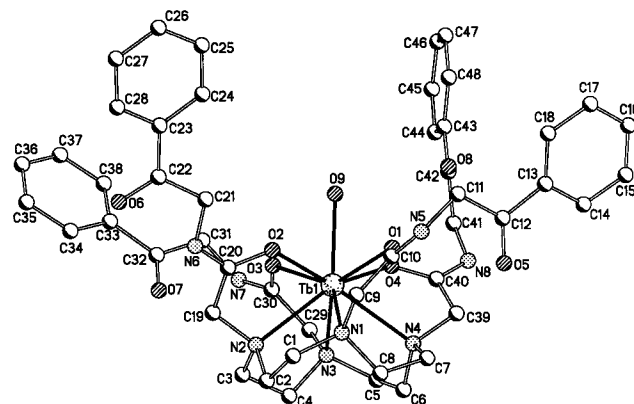
been excited with an energy for which the absorbance is lower than 0.05 to ensure a linear relationship between the emission intensity and the concentration. Since the measurements described here have been performed independently and using several references, their good convergence point to the reported data is taken to be reliable.

X-ray Experimental Section. **TbL5** was crystallized from water. Details about the crystal, data collection, and structure refinement are listed in Table 3. Diffraction data were collected on a mar345 Imaging Plate Detector at 143 K. Data reduction was performed with marHKL release 1.9.1.²² The structure was solved with ab initio direct methods²³ and refined using the full-matrix least-squares on F^2 with all non-H atoms anisotropically defined. H atoms were placed in calculated positions (except those belonging to water molecules, which were not included in the final model) with $U_{\text{iso}} = aU_{\text{eq}}(\text{X})$ (where *a* is 1.2 and X the parent atom).

Structure refinement, molecular graphics, and geometrical calculation were carried out with the SHELXTL software package, release 5.1.²⁴

Results and Discussion

Synthesis of the Ligands and Complexes. Ligands **L5** and **L6** were prepared by reacting cyclen in anhydrous THF

**Figure 2.** Ball-and-stick representation of **TbL5** depicting the cation with its atom-numbering scheme (hydrogen atoms are omitted for the sake of clarity).

containing triethylamine with substituted bromoacetamide, itself obtained from the corresponding amine hydrochloride and bromoacetyl bromide. The overall yields (calculated from the starting commercial products) amount to 28.5% for **L5** (2 steps) and 64% for **L6** (4 steps). Complexes were synthesized in CH₂Cl₂ with triflates as counterions; elemental analyses showed their formula to be Ln(trif)₃L₃·*n*H₂O with *n* = 0–3. The LnL5 complexes are quite soluble in water, while the corresponding ones with **L6** are somewhat less soluble. Complexation by the four amide oxygen atoms is evidenced by the presence of only one C=O (amide) stretching vibration in the IR spectra of the complexes, which is shifted to lower energy by ~30 cm⁻¹ compared to that of the free ligands.

Solid State Structure of TbL5. The compound [Tb(**L5**)-(H₂O)](CF₃SO₃)₃·2H₂O (**7**) crystallizes in the triclinic system, space group *P*1. The asymmetric unit contains one complex molecule, three triflate anions, and two water molecules. The metal ion is nine coordinate, being bound to the four nitrogen atoms of the macrocycle, to the four oxygen atoms of the amide functions, and to a water molecule (Figure 2). The average Tb–X distances (where X is a coordinated atom, Table 4) are comparable to those found in the Eu(III) and Lu(III) complexes with **L2** and **L3**,¹² taking into account ionic radius differences: Tb–N = 2.616(7) Å, Tb–O_{amide} = 2.365(5) Å, and Tb–O_w = 2.437(5) Å. The Tb(III) ion is located between the N₄(cycle) and O₄(amide) planes which are almost parallel, the interplanar angle being 0.8(3)°. The distances from Tb(III) to these planes are 1.573(3) and 0.746(3) Å, respectively. The distance between the trans nitrogen atoms of the macrocycle amounts to 4.171(9) Å between N(1) and N(3) and to 4.189(9) Å between N(2) and N(4). The mean N–Tb–O angle (twist angle, τ) is 39.2°; thus, the coordination polyhedron may be described as a distorted monocapped square antiprism, corresponding to the so-called M form. The mean values of the NCCN and NCCO torsion angles are –58.3(9)° and +25.4(11)°, respectively, and the complex adopts a $\Delta(\lambda\lambda\lambda)$ conformation. A complicated network of hydrogen bonds involving both bound O(9) and interstitial O(19) and O(20) water molecules as well as the four NH and the carbonyl O(8) functions directs the stacking of the molecules in the crystal (Table S1, Supporting

(22) Otwinowski, Z.; Minor, W. *Macromolecular Crystallography, Part A*; Carter, C. W., Jr., Sweet, Eds.; Methods in Enzymology Vol. 276; Academic Press: New York, 1997.

(23) Sheldrick, G. M. *Acta Crystallogr.* **1990**, *A46*, 467.

(24) *SHELXTL release 5.1*; Bruker AXS Inc.: Madison, WI, 1997.

Table 4. Selected Bond Lengths (Å) and Angles (deg) for **7**

Tb(1)–O(4)	2.341(5)	O(9)–Tb(1)–N(3)	128.01(19)
Tb(1)–O(2)	2.358(5)	O(4)–Tb(1)–N(2)	140.1(2)
Tb(1)–O(3)	2.380(5)	O(2)–Tb(1)–N(2)	66.8(2)
Tb(1)–O(1)	2.382(5)	O(3)–Tb(1)–N(2)	74.45(19)
Tb(1)–O(9)	2.437(5)	O(1)–Tb(1)–N(2)	131.69(19)
Tb(1)–N(3)	2.596(7)	O(9)–Tb(1)–N(2)	129.9(2)
Tb(1)–N(2)	2.605(7)	N(3)–Tb(1)–N(2)	68.7(2)
Tb(1)–N(1)	2.625(6)	O(4)–Tb(1)–N(1)	131.7(2)
Tb(1)–N(4)	2.638(6)	O(2)–Tb(1)–N(1)	73.29(19)
O(4)–Tb(1)–O(2)	143.9(2)	O(3)–Tb(1)–N(1)	142.3(2)
O(4)–Tb(1)–O(3)	83.32(19)	O(1)–Tb(1)–N(1)	66.0(2)
O(2)–Tb(1)–O(3)	84.44(18)	O(9)–Tb(1)–N(1)	125.8(2)
O(4)–Tb(1)–O(1)	85.11(19)	N(3)–Tb(1)–N(1)	106.0(2)
O(2)–Tb(1)–O(1)	84.31(19)	N(2)–Tb(1)–N(1)	68.9(2)
O(3)–Tb(1)–O(1)	142.55(19)	O(4)–Tb(1)–N(4)	66.12(19)
O(4)–Tb(1)–O(9)	71.0(2)	O(2)–Tb(1)–N(4)	140.90(19)
O(2)–Tb(1)–O(9)	73.02(19)	O(3)–Tb(1)–N(4)	132.4(2)
O(3)–Tb(1)–O(9)	72.96(19)	O(1)–Tb(1)–N(4)	72.6(2)
O(1)–Tb(1)–O(9)	69.59(18)	O(9)–Tb(1)–N(4)	124.1(2)
O(4)–Tb(1)–N(3)	72.3(2)	N(3)–Tb(1)–N(4)	68.9(2)
O(2)–Tb(1)–N(3)	132.2(2)	N(2)–Tb(1)–N(4)	106.1(2)
O(3)–Tb(1)–N(3)	67.4(2)	N(1)–Tb(1)–N(4)	68.6(2)
O(1)–Tb(1)–N(3)	140.6(2)		

Information). Each NH group interacts with a triflate anion, while the carbonyl group O(8) is linked to O(20). Water molecules display interactions between them and with one triflate anion. The crystal packing consists of a series of dimers linked together by water molecules (Figure S1, Supporting Information), as already observed for other tetraamide complexes,¹² whereas the total network consists of infinite one-dimensional chains. No π -stacking interaction occurs between the aromatic rings.

Structural Properties of EuL5 and EuL6. High-resolution luminescence spectroscopy allows one to investigate the coordination environment of the Eu(III) ion by analyzing the transitions from the 5D_0 level. For **EuL6**, the laser-excited excitation spectrum of the $^5D_0 \leftarrow ^7F_0$ transition, which features a single component for a given chemical environment due to the nondegeneracy of the initial and final electronic states, exhibits one sharp band at $17\,217\text{ cm}^{-1}$ with a full width at half-height (fwhh) equal to 1 cm^{-1} at 13 K. This clearly points to a single, well-defined metal ion site in this compound. The situation for **EuL5** is somewhat different, with a much broader band ($17\,229\text{ cm}^{-1}$, fwhh = 6 cm^{-1}) displaying shoulders on both sides; the broadening is due to a less good quality of the microcrystals while the shoulders may be assigned to vibronic transitions because excitation at these energies yields emission spectra identical to that obtained by exciting at an energy corresponding to the maximum of the $^5D_0 \leftarrow ^7F_0$ transition. Broad band excitation of the $^5L_6 \leftarrow ^7F_{0,1}$ transitions at 13 K yields emission spectra in which the corrected relative intensities for the $^5D_0 \rightarrow ^7F_J$ transitions are 0.10, 1.00, 3.27, and 1.80 (**EuL5**) and 0.14, 1.00, 2.90, and 2.17 (**EuL6**) for $J = 0, 1, 2,$ and $4,$ respectively. The intensity of the $^5D_0 \rightarrow ^7F_0$ transition is fairly large, which is indicative of an axial symmetry.²⁵ Direct laser excitation of the $^5D_0(\text{Eu})$ level results in spectra which may be interpreted as arising from

distorted C_4 symmetry (Figure S2, Supporting Information), in line with the data obtained by X-ray diffraction on a single crystal of the Tb(III) complex. For instance, the $^5D_0 \rightarrow ^7F_1$ transition is composed of three components, two of them being closely spaced for **EuL6** (arising from the splitting of the $^7F_1(\text{E})$ sublevel) while these components are more equally spaced in **EuL5**. From these data, one infers that the coordination polyhedron is more distorted with respect to the idealized C_4 symmetry in the latter compound.

Stability Constant of EuL5. To determine if the bulky substituents grafted on the amide functions have an influence on the stability of the resulting complexes in water, we have determined the stability constant of **EuL5** by competitive spectrophotometric titration with dtma (1,4,7,10-tetrakis-(methylcarbamoylmethyl)-1,4,7,10-tetraazacyclododecane). Preliminary kinetic tests indicated that a solution containing 90% dtma and 10% **L5** (metal-to-ligand ratio = 1:1) reaches thermodynamic equilibrium after 20 days, while a solution containing 10% dtma and 90% **L5** reaches equilibrium after 15 days, which tends to point to a slightly faster formation kinetics with **L5** as compared with dtma.

The competing ligand chosen is one of the few amide derivatives of cyclen for which stability constants have been reported, for example, $\log K(\text{Eu}) = 13.17 \pm 0.04$.¹⁶ The titration was conducted in batch mode, allowing 25 days for equilibration. The solutions contained an equimolar ratio of the two ligands and metal-to-ligand ratios in the range 0–1.5. Factor analysis revealed only two absorbing species in the range 225–300 nm, because dtma and its complexes do not absorb in this spectral range and the fit to the data converged for $\log K(\text{Eu}) = 12.89 \pm 0.15$. That is, the substitution of the pendant arms has only a very little destabilizing effect. This can be explained by the lack of interaction between the arms evidenced in the X-ray crystal structure of **TbL5**.

Photophysical Properties in Aerated Water. The absorption spectra of **L5** and its complexes display two bands at $40\,300$ and $35\,700\text{ cm}^{-1}$ with molar absorption coefficients around $45\,000$ and $6000\text{ M}^{-1}\text{ cm}^{-1}$, respectively (Eu complex, Figure 1). No significant shift occurs upon complexation. We assign these bands to transitions with main $\pi \rightarrow \pi^*$ and $n \rightarrow \pi^*$ character. On the other hand, **L6** and its complexes display only one broad and asymmetric band at $36\,000\text{ cm}^{-1}$, but it is more intense ($\epsilon = 50\,500\text{ M}^{-1}\text{ cm}^{-1}$ for the Eu complex).

Upon excitation of these transitions, no fluorescence is detected at room temperature or at 77 K, but phosphorescence from the triplet states is seen at low temperature, which reveals an efficient intersystem crossing in both ligands (Figure 3). At low temperature, nonradiative deactivation pathways become less probable, so that deactivation of the excited singlet state mainly occurs via the intersystem crossing, the efficacy of which is large and comparable to that reported for cyclen derivatives fitted with an arm bearing a benzophenone chromophore.²⁶ The 0-phonon transitions of the triplet states are located at $24\,550$ (**L5**) and $20\,080$

(25) Bünzli, J.-C. G. In *Lanthanide Probes in Life, Chemical and Earth Sciences. Theory and Practice*; Bünzli, J.-C. G., Choppin, G. R., Eds.; Elsevier Science: Amsterdam, 1989; Chapter 7.

(26) Beeby, A.; Bushby, L. M.; Maffeo, D.; Williams, J. A. G. *J. Chem. Soc., Perkin Trans. 2* **2000**, 1281.

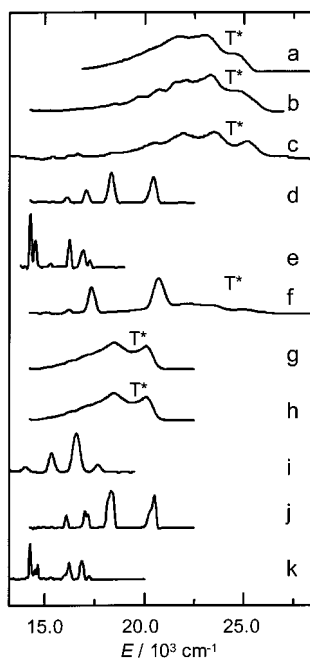


Figure 3. Phosphorescence spectra in frozen acetonitrile (77 K): (a) **L5** (2×10^{-4} M, $\tilde{\nu}_{\text{exc}} = 40\,000\text{ cm}^{-1}$), (b) **LuL5** (2×10^{-4} M, $40\,000\text{ cm}^{-1}$), (c) **SmL5** (5×10^{-4} M, $40\,000\text{ cm}^{-1}$), (d) **TbL5** (1×10^{-5} M, $41\,670\text{ cm}^{-1}$), (e) **EuL5** (1×10^{-5} M, $40\,000\text{ cm}^{-1}$), (f) **DyL5** (1×10^{-5} M, $40\,320\text{ cm}^{-1}$), (g) **L6** (1×10^{-5} M, $28\,570\text{ cm}^{-1}$), (h) **LuL6** (1×10^{-5} M, $33\,330\text{ cm}^{-1}$), (i) **SmL6** (1×10^{-5} M, $33\,330\text{ cm}^{-1}$), (j) **TbL6** (1×10^{-5} M, $33\,330\text{ cm}^{-1}$), (k) **EuL6** (1×10^{-5} M, $34\,720\text{ cm}^{-1}$).

cm^{-1} (**L6**). The emission spectra of the nonluminescent Lu(III) complexes have also been recorded to evaluate the influence of the coordination. As for the free ligands, the singlet states could not be located. The energy of the 0-phonon transitions of the triplet states amounts to $25\,300$ and $20\,800\text{ cm}^{-1}$ for **LuL5** and **LuL6**, respectively, close to the values reported for the calixarene complexes.¹³ In addition, time-resolved luminescence spectroscopy allowed us to locate the triplet state of **SmL5** and **DyL5** because transfer onto the corresponding ions is incomplete, allowing for residual triplet state emission. That Dy(III) is not sensitized by **L5** is somewhat surprising because the energy difference between its excited level $^4\text{F}_{9/2}$ and the ligand triplet state (3400 cm^{-1}) is more favorable for an efficient energy transfer than that in the Eu(III) complex (7000 cm^{-1} for $^5\text{D}_0$). However, the selection rule on ΔJ ^{27,28} is less favorable for Dy(III) than for Eu(III), and, as a consequence, the energy transfer from the ligand triplet state to the $^5\text{D}_0$ level is allowed, while it is forbidden to the $^4\text{F}_{9/2}$ state. Moreover, deactivation of the metal ion excited states by OH vibrations has also to be taken into account (see later). Similar considerations hold for **SmL5**.

Compared with **LnL5**, the triplet state of the complexes formed with **L6** is lower in energy and back transfer processes are likely to happen, particularly for Tb(III) for

Table 5. Largest Quantum Yields Obtained in Aerated Water, Decay Rate Constants of the $^5\text{D}_4(\text{Tb})$, $^5\text{D}_0(\text{Eu})$, and $^4\text{G}_{5/2}(\text{Sm})$ Excited Levels in Water and Deuterated Water, and Hydration Numbers q

compd	$E_{\text{exc}}/\text{cm}^{-1}$	$\Phi_{\text{abs}}/\%$	$k(\text{H}_2\text{O})/\text{ms}^{-1}$	$k(\text{D}_2\text{O})/\text{ms}^{-1}$	q^a
SmL5	34 722	0.4	<i>b</i>	<i>b</i>	<i>b</i>
EuL5	34 722	5.5	1.67	0.56	0.7
TbL5	40 323	23.1	0.53	0.34	0.7
DyL5	40 323	0.05	<i>b</i>	<i>b</i>	<i>b</i>
SmL6	34 722	0.7	100	16.7	1.0
EuL6	34 722	24.7	1.59	0.68	0.4
TbL6	34 720	1.0	<i>b</i>	<i>b</i>	<i>b</i>

^a Calculated using the following equations: $q = 1.2(\Delta k - \Delta k_{\text{corr}} - 0.075x)$ for Eu(III), and $q = 5(\Delta k - \Delta k_{\text{corr}})$ for Tb(III), where $\Delta k = k(\text{H}_2\text{O}) - k(\text{D}_2\text{O})$, $\Delta k_{\text{corr}} = 0.25$ (Eu) and 0.06 ms^{-1} (Tb), and x is the number of NH oscillators;²⁹ $q = 0.026k(\text{H}_2\text{O}) - 1.6$ for Sm(III).³⁰ ^b Not measured.

which $\Delta E(^3\pi\pi^* - ^5\text{D}_4)$ amounts to only 300 cm^{-1} . An exponential decay of the radiative deactivation rate with increasing temperature is indeed observed (Figure S3, Supporting Information), the lifetime decaying very rapidly up to 100 K .

The quantum yields of the complexes with **L5** ($\text{Ln} = \text{Sm}, \text{Eu}, \text{Tb}, \text{Dy}$) and **L6** ($\text{Ln} = \text{Sm}, \text{Eu}, \text{Tb}$) have been determined upon ligand excitation in aerated water. Whenever possible, data have been measured using several different references, and the influence of the excitation energy has also been examined. Indeed, ligand-to-metal energy transfer processes are rather complex,²⁸ and both the excited singlet and triplet states may transfer energy onto the lanthanide ion, so that the quantum yield possibly will change depending on which ligand state is excited. Moreover, to avoid correction problems, both the sample and the reference have been excited at the same energy, which sometimes may not be optimum for one of them. For a given excitation energy, the data reported in Tables 1 and 2 are coherent from one reference to the other, with two exceptions for which the difference in the absolute quantum yield exceeds the experimental error that, we believe, is on the order of $\pm 20\%$ given the precaution taken. These exceptions may be explained by nonideal experimental conditions, that is, a particularly low absorbance of the reference used, which becomes very difficult to measure. Moreover, an important result is that excitation of the lower singlet state of the ligand produces always a better quantum yield of the metal-centered luminescence. This can be traced back to a smaller energy gap between the ligand excited state(s) and the acceptor and/or luminescent state(s) of the metal ion. When a ligand state with higher energy is excited, more energy is lost during the migration onto the luminescent excited state of the metal ion through more numerous nonradiative deexcitation processes.

Ligand **L5** is a very good sensitizer of the Tb(III) luminescence and a good sensitizer of the Eu(III) luminescence, while it also sensitizes the otherwise poorly luminescent Sm(III) and Dy(III) ions. Table 5 summarizes the quantum yields obtained under the best conditions and lists the radiative decay rate constants of the metal excited states measured both in water and deuterated water, from which hydration numbers can be obtained.^{29,30} For the Eu(III) and Tb(III) complexes with **L5**, q amounts to 0.7, close to the

(27) de Sá, G. F.; Malta, O. L.; Donega, C. D.; Simas, A. M.; Longo, R. L.; Santa-Cruz, P. A.; da Silva, E. F. *Coord. Chem. Rev.* **2000**, *196*, 165.

(28) Gonçalves e Silva, F. R.; Longo, R. L.; Malta, O. L.; Piguet, C.; Bünzli, J.-C. G. *Phys. Chem. Phys.* **2000**, *2*, 5400. Gonçalves e Silva, F. R.; Malta, O. L.; Reinhard, C.; Güdel, H.-U.; Piguet, C.; Moser, J. E.; Bünzli, J.-C. G. *J. Phys. Chem. B* **2002**, *106*, 1670.

expected value of 1. Therefore, in addition to the energy factors and selection rules discussed previously, efficient deactivation through OH vibration due to a small gap between the excited and ground state of Sm(III) and Dy(III) certainly contributes to the weak luminescence of these ions. The quantum yield for the Tb(III) compound is quite large, 23.1%, because of both an efficient intersystem crossing and energy transfer process, and also because of a good protection of the metal ion from vibronic deactivation by solvent molecules.

On the other hand, ligand **L6** does not sensitize efficiently the luminescence of Tb(III), because of the back transfer process mentioned earlier, but is an excellent sensitizer of the Eu(III) luminescence and a fair sensitizer of the Sm(III) luminescence. The value found for **EuL6** (24.7%) is among the largest reported in water for a europium complex belonging to this class of compounds. The value of 0.7% for **SmL6** is also interesting because the absolute quantum yields for Sm(III) rarely exceed 2% in aqueous medium.³¹ The best quantum yields reported to date for terbium and europium cyclen derivatives are 49.0%³² and 9.5%,²⁶ with Ph-*p*-CO₂CH₃ and C₆H₄COPh groups as sensitizers, respectively, and therefore, **EuL6** is the most luminescent Eu(III) containing cyclen derivative reported so far.

Conclusion

Ligands **L5** and **L6** lead to stable complexes [LnL(H₂O)]³⁺ in water. The Tb(III) and Eu(III) complexes with **L5** and **L6**, respectively, are good candidates as luminescent stains, as well as **EuL5**, because for instance, some commercial fluoroimmunoassays are based on far less luminescent Eu(III) probes (cf. the quantum yield of [Eu(bpy·bpy·bpy)]³⁺ which amounts to only 2%).³³ The quantum yields are shown to depend on the excitation energy: when a ligand singlet

state with higher energy is excited, an important loss of energy occurs during the energy migration to the luminescent level of the metal ion, leading to less efficient antenna effect. However, because the molar absorption coefficient is also larger for the more energetic transition, the overall efficacy of the luminescent macrocyclic compounds may remain large, which means that these potential probes can be excited in a fairly broad spectral range. These results are promising because the described compounds fulfill two essential criteria for potential use in fluoroimmunoassays, namely, large stability and intense metal luminescence in water. The present study also demonstrates that phenacyl and 4-phenylphenacyl chromophoric moieties are well suited for designing efficient UV-to-visible light converters because of both efficient intersystem crossing and ligand-to-metal energy transfer. This opens the way for the use of these potential probes in submicromolar concentration, an asset in the analysis of biological material. Furthermore, we have demonstrated that the luminescence of Sm(III) and Dy(III) is also sensitized, which is interesting in view of the development of multiple fluoroimmunoassays. Modification of **L5** and **L6** for allowing a coupling to biological materials is presently underway in our laboratories.

Acknowledgment. We thank the Swiss National Science Foundation, the Swiss Federal Office for Science and Education (COST project D18, contract C00.0030) for funding this research project, the Fondation Herbette (Lausanne) for spectroscopic equipment, and N. André for his assistance in using the Specfit program.

Supporting Information Available: Table and figures describing the hydrogen bond network in [Tb(**L5**)(H₂O)](CF₃SO₃)·2H₂O, high-resolution emission spectra of the ³D₀ → ⁷F_{*j*} transitions in **EuL5** and **EuL6** at 13 K, and Arrhenius analysis of the energy back transfer in a microcrystalline sample of **TbL6**. Crystallographic data in CIF format. This material is available free of charge via the Internet at <http://pubs.acs.org>.

IC011121I

- (29) Beeby, A.; Clarkson, I. M.; Dickins, R. S.; Faulkner, S.; Parker, D.; Royle, L.; de Sousa, A. S.; Williams, J. A. G.; Woods, M. *J. Chem. Soc., Perkin Trans. 2* **1999**, 493.
- (30) Kimura, T.; Kato, Y. *J. Alloys Compd.* **1995**, 225, 284.
- (31) Hemmilä, I.; Ståhlberg, T.; Mottram, P. *Bioanalytical Applications of Labeling Technologies*; Wallac Oy: Turku, Finland, 1995.
- (32) Dickins, R. S.; Howard, J. A. K.; Maupin, C. L.; Moloney, J. M.; Parker, D.; Riehl, J. P.; Siligardi, G.; Williams, J. A. G. *Chem.—Eur. J.* **1999**, 5, 1095.

- (33) Mathis, G. In *Rare Earths*; Saez Puche, R., Caro, P., Eds.; Editorial Complutense: Madrid, 1998.